

Polarity-dependent reversible resistance switching in Ge–Sb–Te phase-change thin films

Ramanathaswamy Pandian, Bart J. Kooi,^{a)} George Palasantzas, and Jeff T. M. De Hosson
Department of Applied Physics, Zernike Institute for Advanced Materials, and the Netherlands Institute for Metals Research, University of Groningen, Nijenborgh 4, 9747 AG Groningen, the Netherlands

Andrew Pauza

Plasmon Data Systems Ltd., Whiting Way, Melbourn Royston, Hertsfordshire, SG8 6EN, United Kingdom

(Received 19 July 2007; accepted 21 September 2007; published online 8 October 2007)

In this paper, we demonstrate reversible resistance switching in a capacitorlike cell using a Ge–Sb–Te film that does not rely on amorphous-crystalline phase change. The polarity of the applied electric field switches the cell resistance between lower- and higher-resistance states, as was observed in current-voltage characteristics. Moreover, voltage pulses less than 1.25 V showed this switching within time scales of microseconds with more than 40% contrast between the resistance states. The latter are found to be nonvolatile for months. The switching could also be achieved at nanoscales with atomic force microscopy with a better resistance contrast of three orders of magnitude. © 2007 American Institute of Physics. [DOI: [10.1063/1.2798242](https://doi.org/10.1063/1.2798242)]

For next generation nonvolatile memories, several random access memory (RAM) technologies have been proposed, e.g., based on magnetoresistance (MRAM),¹ ferroelectricity (FRAM),² phase-change (PRAM),³ and electrical-resistance (RRAM).^{4–13} Full understanding of the switching mechanisms in RRAM, mostly voltage-polarity dependent, is still lacking. Various models have been proposed, e.g., based on trap-controlled space-charge-limited current,⁴ charge-trapping-defect states inside the band gap,⁵ charge-trap states at metal/oxide interfaces with a change of Schottky-like barrier,⁶ electric-pulse-induced vacancy/ion motion,⁷ and filamentary conduction.^{8–13} In contrast, PRAM is based on the resistance switching caused by amorphous-crystalline phase change and is not voltage-polarity dependent.

Up to now, phase-change and polarity-dependent resistance (PDR, non-phase-change) switchings in chalcogenides were considered independently.¹⁴ Resistance switching based on phase change will generally require a higher operating voltage than that for PDR switching. Moreover, the phase-change process could possibly suffer from fatigue due to volumetric changes involved, and from segregation or phase separation.^{15–17} PDR switching in Ag-free chalcogenides, such as in Ge–Sb–Te system most commonly used in phase-change data storage, has not yet been demonstrated. Ag–In–Sb–Te is the only phase-change material for which PDR switching was reported.¹³ However, this system showed a high threshold voltage (>10 V), which is a significant drawback. In this paper, we demonstrate that PDR switching can be achieved with Ge–Sb–Te, both on macroscopic and nanometer length scales using low voltages (0.4–1.25 V) incapable of inducing amorphous-crystalline phase change in our system.

The samples consist of 20 or 40 nm thick Sb-excess $\text{Ge}_2\text{Sb}_{2+x}\text{Te}_5$ (GST) phase-change films on 100 nm thick Mo bottom electrodes on Si substrates. Mo and amorphous GST were deposited *in situ* by dc magnetron sputtering. Ag or Au was used as top electrode. Such capacitorlike devices shown in Fig. 1(a) were used to examine the PDR switching via I - V

measurements using a Keithley 2601 source meter with a voltage sweep rate of ~ 0.8 V/s. This switching was also tested with voltage pulses for repeated cycles using a pulse generator. Finally, to investigate switching at nanoscale, conductive atomic force microscopy (C-AFM) (Veeco Dimension-3100) was used. In this case, a highly conductive (Pt/Ir coated) tip serves as top electrode. The local conductivity of the sample is read from the current image. All measurements were made in air and at room temperature.

A typical macroscopic I - V characteristic of a GST film is shown in Fig. 1(b). Before the measurements, the material between the electrodes was crystallized by sweeping the voltage from zero to a value higher than the threshold voltage for crystallization. Hence, the sample is initially in the lower-resistance state (LRS). When sweeping the voltage from zero in the negative direction with respect to the bottom electrode, a linear I - V behavior is observed for $V > -0.4$. Below this threshold voltage (V_{th}) the sample switches to an about five times higher-resistance state (HRS) and remains there when sweeping the voltage back to positive values until reaching a bias voltage of +0.4, above which the resistance of the sample is restored to the initial LRS. This I - V characteristic, with two different resistance states, clearly exhibits PDR-switching behavior. This intrinsic memory effect is stable and reproducible within ± 0.4 V. The imposed cutoff for large currents (>40 mA) in Fig. 1(b) is to prevent sample damage. According to the I - V characteristics, the resistance states are nonvolatile and could be read with lower bias voltages ($\ll V_{\text{th}}$) of either polarity. PDR switching without first crystallizing Ge–Sb–Te turned out impossible.

Using voltage pulses for the switching procedure includes the advantages of fast device operation and reduced thermal effects or damage. Measurements using different voltage pulses for a number of cycles on different samples are depicted in Fig. 1(c); on the left, sample 1 shows switching with 500 μs pulses at ± 1.1 V, and on the right, the response of sample 2 to 1 μs pulses at ± 1.25 V is shown. Note that the effective cell area of sample 2 compared to sample 1 is larger. A negative pulse, causing LRS \rightarrow HRS switching, is equivalent to a set/write process giving the on state. The on

^{a)}Electronic mail: b.j.kooi@rug.nl

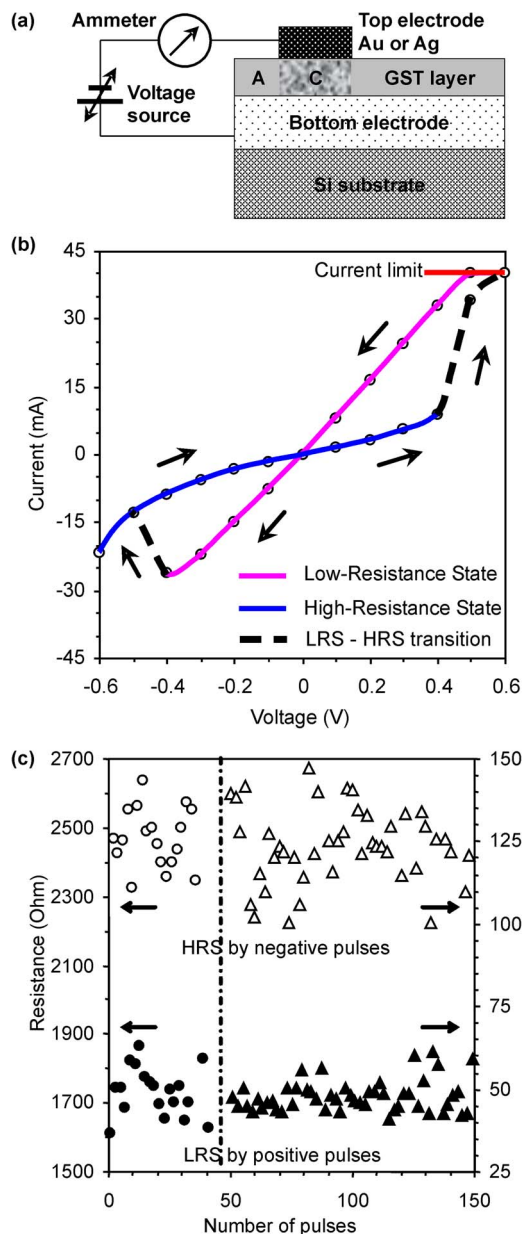


FIG. 1. (Color online) (a) Schematic of the prototype cell structure, where A and C refer to amorphous and polycrystalline GST layer, respectively. (b) Memory switching I - V behavior of the cell. (c) Two-state resistance switching behavior in a pulse-mode; circular symbols on the left side indicate sample 1 switched by ± 1.1 V, 500 μ s pulses, and triangular symbols on the right side indicate sample 2 switched by ± 1.25 V, 1 μ s pulses.

state was found to be nonvolatile for more than a month. By a positive pulse, the LRS is recovered; i.e., the information is erased and this reset process recovers the off state. Between each write/erase pulse, the resistance state of the device was read with a voltage < 0.1 V for ~ 20 ms duration. The resistance switching was stable and reproducible with a contrast of $R_{\text{HRS-LRS}}$ more than 40% for sample 1 and about 150% for sample 2.

Memory switching at nanoscales is essential to obtain high data-storage densities. In recent years, a strong impetus in this direction has been given by AFM nanolithography.¹⁸ Therefore, we explored the resistance switching at nanoscales by C-AFM [Fig. 2(a)]. The AFM tip, with radius > 50 nm, was used as top electrode by switching an area, 500×500 nm², of the GST layer. Prior to switching experi-

ments, this area was crystallized by a large voltage (5 V) between the tip and the bottom electrodes with an electrical current of > 10 nA.

During resistance switching with ± 1 V between the grounded tip and bottom electrodes, simultaneous measurement of current flow through the tip allowed mapping the resistance state of the mark. The LRS is shown in Fig. 2(b) for +1 V, and the HRS upon a SET operation with -1 V is shown in Fig. 2(c). The HRS of the mark is electrically indistinguishable from the surrounding amorphous phase, because the current flow across both the amorphous and HRS crystalline phases is < 5 pA, and, thus, lower than the detection limit of the C-AFM setup. By a reset operation with +1 V, the LRS of the mark was recovered as shown in Fig. 2(d). The current contrast between HRS and LRS reaches values beyond 2000 pA.

In Figs. 2(b) and 2(d), it can be seen that the electrical conductivity of the crystallized area is not uniform. A considerable area fraction is still in a HRS, where it should be homogeneous in a LRS. This is attributed to several factors, e.g., an incomplete crystallization by the tip, an improper tip-sample electrical contact due to relative fast tip scanning, surface roughness of the sample, and removal of the conductive coating from the tip. Our experiments prove that the switching is not limited by the switching area and probably the electrode type also, but the switching speed is limited by a few experimental constraints, i.e., AFM scanning speed, and pulse-shape loss due to the large capacitance of our non-optimized test structures. Switching in nanoscale areas is definitely possible as already shown in Fig. 2. It was also found later that switching of sample 2 with ± 1 V pulses of 500 ns was feasible up to 400 cycles with a contrast of 100%, indicating that the switching limits have not yet been reached.

The resistance switching driven by the polarity of the applied electric field can be related to the solid-state electrolytic behavior of the chalcogenide. When it is subjected to an electric field, electrochemical reactions near the electrodes lead to ionic conduction. If the electric field is sufficiently strong, electrically conductive filamentary pathways form between the electrodes leading to a LRS, and if the polarity is reversed, the pre-existing paths became discontinuous due to ion migration in the opposite direction resulting in a HRS. In literature, chalcogenides showing this behavior include Ag-S,⁹ Cu-S,¹⁰ Ag-Ge-Se,¹¹ Ag-Ge-Te,¹² and Ag-In-Sb-Te,¹³ where the LRS and the HRS are results of the formation and rupture of Ag filaments. A similar electrolytic switching mechanism probably holds for our Sb-excess GST chalcogenide material. In this case, conductive Sb instead of Ag filaments can be formed and dissolved in an amorphous phase that still persists with a small volume fraction when the GST crystallites are formed.

This mechanism is favored by the facts that (i) (fast) crystallization of GST with excess Sb leads to a phase separation, where the Ge₂Sb₂Te₅ nanocrystals form with the excess Sb in the amorphous phase at grain boundaries,¹⁵ and (ii) cross-sectional transmission electron microscopy (TEM) studies showed that in GST films, a strong tendency exists to form crystallites near the film surface leaving some amorphous volume near the film-substrate interface.^{17,19} Metallic Sb is also several orders of magnitude more conductive than Ge and Te in GST. Cross-sectional TEM studies are in progress to investigate these issues in the GST system. All rights reserved. This article is copyrighted as indicated in the article. Reuse of AIP content is subject to the terms at: <http://scitation.org/termsconditions>. Downloaded to IP: 129.125.25.39. Redistribution subject to AIP license or copyright; see <http://apl.aip.org/apl/copyright.jsp>

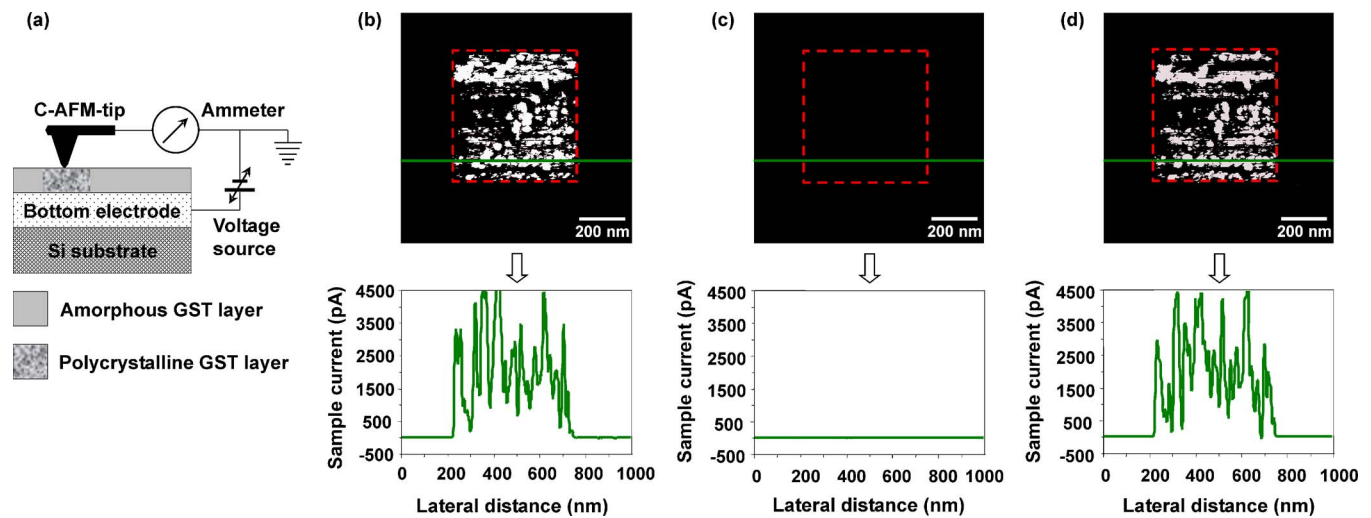


FIG. 2. (Color online) PDR switching at nanoscales using a C-AFM. (a) Sample structure and AFM experimental setup. (b) Current image and current profile recorded with +1 V bias to the bottom electrode showing the LRS of the crystalline area (dashed square). (c) Current image, recorded with -1 V bias during the set operation, and current profile showing the system's HRS (on state, not distinguishable from the surrounding amorphous phase). (d) Current image and current profile showing the reproducibility of the initial LRS upon the reset operation with +1 V bias.

though, currently, we cannot fully exclude an electrode-induced switching mechanism, the previously proposed mechanism appears to be more favorable.

Striking in our experiments is that $R_{\text{HRS-LRS}}$ for a smaller switching area is larger (compare Figs. 1 and 2). Macroscopic (millimeter) contacts on 20 or 40 nm films will suffer more from potential current-leakage paths in the film and will thus decrease the HRS. Furthermore, it is likely that within smaller areas, the conducting filaments are more effectively switched (i.e., formed or ruptured) compared to the larger areas and will thus increase $R_{\text{HRS-LRS}}$. Down scaling is thus advantageous, and this is an important finding for applications.

In conclusion, we demonstrated polarity-dependent resistance switching in crystallized Sb-excess $\text{Ge}_2\text{Sb}_{2+x}\text{Te}_5$ films from macro- to nanoscales. Voltage pulses showed this switching within time scales of microseconds with more than 40% contrast between the resistance states for macroscopic contacts. Moreover, using conductive atomic force microscopy, switching was also possible at nanoscales with a better resistance contrast of more than three orders of magnitude. Notably, the switching (write/erase) voltage of ± 1.1 V is fairly small compared to those used in current ferroelectric and flash memories, and is compatible with future microelectronic and data-storage systems. Our study shows conclusively that in a single material phase-change and polarity-dependent switching can be combined.

The project has been funded by the Zernike Institute for Advanced Materials. Thanks are due to Pim van den Dool for technical assistance.

¹G. A. Prinz, *Science* **282**, 1660 (1998).

²G. R. Fox, F. Chu, and T. Davenport, *J. Vac. Sci. Technol. B* **19**, 1967 (2001).

³S. R. Ovshinsky, *Phys. Rev. Lett.* **21**, 1450 (1968); K. Nakayama, K. Kojima, F. Hayakawa, Y. Imai, A. Kitagawa, and M. Suzuki, *Jpn. J. Appl.*

Phys., Part 1 **39**, 6157 (2000); S. Lai and T. Lowrey, *Tech. Dig. - Int. Electron Devices Meet.* **36**, 803 (2001); F. Pellizzer *et al.*, *Proceedings of the 2004 IEEE Symposium on VLSI Technology, Digest of Technical Papers* (unpublished), Paper No. 3.1, p. 18; S. H. Lee, Y. N. Hwang, S. Y. Lee, K. C. Ryoo, S. J. Ahn, H. C. Koo, C. W. Jeong, Y.-T. Kim, G. H. Koh, G. T. Jeong, H. S. Jeong, and K. Kim, *Proceedings of the 2004 IEEE Symposium on VLSI Technology, Digest of Technical Papers* (unpublished), p. 20.

⁴K. L. Chopra, *J. Appl. Phys.* **36**, 184 (1965).

⁵A. Beck, J. G. Bednorz, Ch. Gerber, C. Rossel, and D. Widmer, *Appl. Phys. Lett.* **77**, 139 (2000).

⁶A. Sawa, T. Fujii, M. Kawasaki, and Y. Tokura, *Appl. Phys. Lett.* **85**, 4073 (2004).

⁷X. Chen, N. Wu, J. Strozier, and A. Ignatiev, *Appl. Phys. Lett.* **89**, 063507 (2006); A. Ignatiev, N. J. Wu, X. Chen, S. Q. Liu, C. Papagianni, and J. Strozier, *Phys. Status Solidi B* **243**, 2089 (2006).

⁸K. Szot, R. Dittmann, W. Speier, and R. Waser, *Phys. Status Solidi (RRL)* **1**, R86 (2007).

⁹Y. Hirose and H. Hirose, *J. Appl. Phys.* **47**, 2767 (1976); K. Terabe, T. Hasegawa, T. Nakayama, and M. Aono, *Nature (London)* **433**, 47 (2005).

¹⁰T. Sakamoto, *NEC J. Adv. Tech.* **2**, 260 (2005).

¹¹M. N. Kozicki, M. Park, and M. Mitkova, *IEEE Trans. Nanotechnol.* **4**, 331 (2005).

¹²C.-J. Kim and S.-G. Yoon, *J. Vac. Sci. Technol. B* **24**, 721 (2006).

¹³Y. Yin, H. Sone, and S. Hosaka, *Jpn. J. Appl. Phys.*, Part 1 **45**, 4951 (2006).

¹⁴A. L. Greer and N. Mathur, *Nature (London)* **437**, 1246 (2005).

¹⁵N. Yamada and T. Matsunaga, *J. Appl. Phys.* **88**, 7020 (2000).

¹⁶Y. Kim, S. A. Park, J. H. Baeck, M. K. Noh, K. Jeong, M.-H. Cho, H. M. Park, M. K. Lee, E. J. Jeong, and D.-H. Ko, and H. J. Shin, *J. Vac. Sci. Technol. A* **24**, 929 (2006); L. K. Elbaum, C. Cabral, K. N. Chen, M. Copel, D. W. Abraham, K. B. Reuter, S. M. Rossnagel, J. Bruley, and V. R. Deline, *Appl. Phys. Lett.* **90**, 141902 (2007).

¹⁷S.-M. Yoon, K.-J. Choi, N.-Y. Lee, S.-Y. Lee, Y.-S. Park, and B.-G. Yu, *Jpn. J. Appl. Phys.*, Part 2 **46**, L99 (2007).

¹⁸S. Gidon, O. Lemonnier, B. Rolland, O. Bichet, C. Dressler, and Y. Samson, *Appl. Phys. Lett.* **85**, 6392 (2004); K. Tanaka, *J. Non-Cryst. Solids* **353**, 1899 (2007); C. D. Wright, M. Armand, and M. M. Aziz, *J. Hist. Astron.* **5**, 50 (2006).

¹⁹J. A. Kalb, C. Y. Wen, F. Spaepen, H. Dieker, and M. Wuttig, *J. Appl. Phys.* **98**, 054902 (2005); T. H. Jeong, M. R. Kim, and H. Seo, *ibid.* **86**, 774 (1999).